Electronic Supplementary Information

Triple-Shelled NiMn$_2$O$_4$ Hollow Spheres as an Efficient Catalyst for Low-Temperature Selective Catalytic Reduction of NO$_x$ with NH$_3$

Yanling Han[#], Jincheng Mu[#], Xinyong Li*, Jinsuo Gao*, Shiying Fan, Feng Tan and Qidong Zhao

Key Laboratory of Industrial Ecology and Environmental Engineering (MOE), School of Environmental Science and Technology, Dalian University of Technology, Linggong Road 2, Dalian 116024, China.

[#] The authors contributed equally to this work.

* To whom correspondence should be addressed. E-mail: xyli@dlut.edu.cn, jsgao@dlut.edu.cn

1. Experimental

1.1. Catalyst preparation

$NiMn_2O_4$ with triple-layer shell was synthesized by a solvothermal method.[1, 2] Typically, 16 mL glycerol was first mixed with 80 mL isopropanol. Then 0.25 mmol $Ni(NO_3)_2·6H_2O$ and 0.5 mmol $Mn(NO_3)_2·6H_2O$ were added into mixture under constant stirring. After becoming homogeneous solution, the mixture was transferred into a 100 mL sealed Teflon-lined autoclave. Next, the mixture was placed in an oven of 180 °C for 6 h followed by filtration, washing with ethanol and dried at 60 °C to obtain NiMn-glycerateand sphere precursors. Finally, the as-synthesized NiMn-glycerate was calcined under 350 °C for 2 h at a rate of 1 °C/min and hollow $NiMn_2O_4$ with triple shells could be obtained (denoted as $NiMn_2O_4$-S). For comparison, an $NiMn_2O_4$ particle sample was prepared by a co-precipitation method.[3] For this synthesis, aqueous ammonia (25 wt%, 20 mL) was rapidly dropped into a mixture of aqueous $Mn(NO_3)_2$ solution (0.2M, 50 mL) and aqueous $Ni(NO_3)_2$ solution (0.2 M, 25 mL) at room temperature. After the mixture was stirred for 2 h, the solvent was evaporated off at 110 °C. The resultant powder was calcined at 350 °C for 2 h to obtain the $NiMn_2O_4$ particles (denoted as $NiMn_2O_4$-P).

1.2. Catalyst characterization

Thermogravimetry (TG) analysis was obtained from the instrument (EXSTAR 6300) produced by Japan Seiko instruments co., ltd. In the air, the sample underwent heat treatment from room temperature to 500 °C at the rate of 10 °C/min. X-ray

diffraction (XRD) patterns were performed on a D/Max 2400 X-ray diffractometer from Japan Rigaku Industrial Corporation, selecting 10° to 80° as scanning angle testing on 40 kV voltage and 100 mA electric current. N_2 adsorption-desorption isotherms are collected from a physical adsorption instrument (Quadrasorb SI) at 77 K after pretreated at 473 K for 3 h, and the specific surface areas of the samples were determined by using the Brunauer-Emmett-Teller (BET) method and the pore volume and average pore diameters were measured from desorption branch of the isotherms using the Barrett-Joyner-Halenda (BJH) method. Scanning electron microscope (SEM) was performed on a Hitachi SU8010 apparatus from Japan, and transmission electron microscope (TEM) images were obtained from the instrument that is FEI Tecnai G20 from America. Before SEM and TEM analysis, the sample diluted in ethanol solution to from uniform suspension. Temperature-programmed reduction by hydrogen (H_2-TPR) was implemented on a Quantachrom automated chemisorption analyzer with 30 mg of each catalyst. Before experiment, the catalyst was pretreated in a He stream at 300 ^{o}C for 30 min and then cooled to room temperature. By switching to 10 vol. % H_2 in He flow, TPR experiment was carried out in the range of 50−900 ^{o}C with a ramping rate of 10 ^{o}C·min^{-1} and monitored online by TCD detector. Temperature-programmed desorption of NH_3 (NH_3-TPD) was also tested on the same instrument with 30 mg of sample. After pretreatment (He flow, 300 ^{o}C for 30 min) and adsorption of NH_3 (10 vol. % NH_3 with He, room temperature for 90 min), TPD experiment was performed in He flow from 50 to 600 ^{o}C with a heat rate of 10 ^{o}C·min^{-1}. X-ray photoelectron spectra (XPS) were collected on a Thermo ESCALAB 250XI multifunctional imaging electron

spectrometer using a monochromatic Al Ka radiation, and the binding energies of Ni

2p, Mn 2p, and O 1s were calibrated using the C 1s peak (BE = 284.6 eV) as standard.

1.3. Activity measurements

The NH$_3$-SCR catalytic performance of the catalyst was tested in a fixed-bed quartz

U-type tube reactor (i.d., 4 mm) with 0.20 g sample that was pressed into pieces. The

reaction temperature was from 50 °C to 300 °C and the composition of simulated gas is

500 ppm NH$_3$, 500 ppm NO, 10 vol% O$_2$ with Ar balanced (GHSV = 68000 h^{-1}). The

concentrations of NO and NO$_2$ in both inlet and outlet were measured by an online gas

analyzer (Testo 350). NO$_x$ conversions of the NH$_3$-SCR reaction at different

temperatures could be calculated through the following formula.

$$\text{NO}_x \text{ conversion (\%)} = \frac{[\text{NO}_x]_{\text{in}} - [\text{NO}_x]_{\text{out}}}{[\text{NO}_x]_{\text{in}}} \times 100\%$$

Where the [NO$_x$] = [NO] + [NO$_2$].

Table S1 The physical and chemical characteristics of NiMn$_2$O$_4$-S and NiMn$_2$O$_4$-P catalysts

Sample	BET specific surface area (m^2·g^{-1})	Pore diameter (nm)	Pore volume (cm^3·g^{-1})	NH$_3$-TPD integral area (a.u.)	H$_2$-TPR integral area (a.u.)
NiMn$_2$O$_4$-S	165.3	3.84	0.29	8102.7	16568.8
NiMn$_2$O$_4$-P	45.4	3.77	0.24	2989.1	14526.9

Table S2 XPS results of $NiMn_2O_4$-S and $NiMn_2O_4$-P catalysts

Sample	Mn^{4+}/Mn^{3+}	$O_\alpha/(O_\alpha + O_\beta)$	Ni^{2+}/Ni^{3+}
$NiMn_2O_4$-S	1.51	0.57	1.01
$NiMn_2O_4$-P	0.60	0.39	0.89

Table S3 Comparison of NH$_3$-SCR performance over typical Mn-based catalysts with NiMn$_2$O$_4$-S catalyst

Catalyst	Reaction condition	C (T/$^\circ$C)^a	Temperature window ($^\circ$C)	Reference
NiMn$_2$O$_4$-S	[NO] = [NH$_3$] = 500 ppm, [O$_2$] = 5 vol.%, GHSV = 68000 h^{-1}	100% (125)	100−225	This work
Mn/Hombikat TiO$_2$	[NO] = [NH$_3$] = 2000 ppm, [O$_2$] = 2 vol.%, GHSV = 12000 h^{-1}	100% (140)	--	4
20% Mn/TiO$_2$	[NO] = [NH$_3$] = 2000 ppm, [O$_2$] = 2 vol.%, GHSV = 50000 h^{-1}	100% (120)	--	5
16.7% Mn/TiO$_2$	[NO] = [NH$_3$] = 400 ppm, [O$_2$] = 2 vol.%, GHSV = 50000 h^{-1}	95% (175)	--	6
Mn–Ni(0.4)/TiO$_2$	[NO] = [NH$_3$] = 400 ppm, [O$_2$] = 2 vol.%, GHSV = 50000 h^{-1}	100% (200)	200−240	7, 8
Mn–Ce/TiO$_2$−Hk	[NO] = 900 ppm, [NO$_2$] = 100 ppm, [NH$_3$] = 1000 ppm, [O$_2$] = 10 vol.%, GHSV = 80000 h^{-1}	93% (100)	100−200	9
Mn(0.25)/TNT-Hombikat	[NO] = 900 ppm, [NO$_2$] = 100 ppm, [NH$_3$] = 1000 ppm, [O$_2$] = 10 vol.%, GHSV = 80000 h^{-1}	98% (100)	100−280	10
Mn$_x$Co$_{3-x}$O$_4$ nanocages	[NO] = [NH$_3$] = 500 ppm, [O$_2$] = 3 vol.%, GHSV = 38000 h^{-1}	100% (150)	150−350	11
CuMn$_2$O$_4$	[NO] = 498 ppm, [NH$_3$] = 500 ppm, [O$_2$] = 3 vol.%, GHSV = 90000 h^{-1}	100% (250)	--	3
Ni(0.4)-MnO$_x$	[NO] = [NH$_3$] = 500 ppm, [O$_2$] = 5 vol.%, GHSV = 64000 h^{-1}	100% (150)	120−240	12

^{a} C: NO$_x$ conversion, T: the reaction temperature that achieved this NO$_x$ conversion.
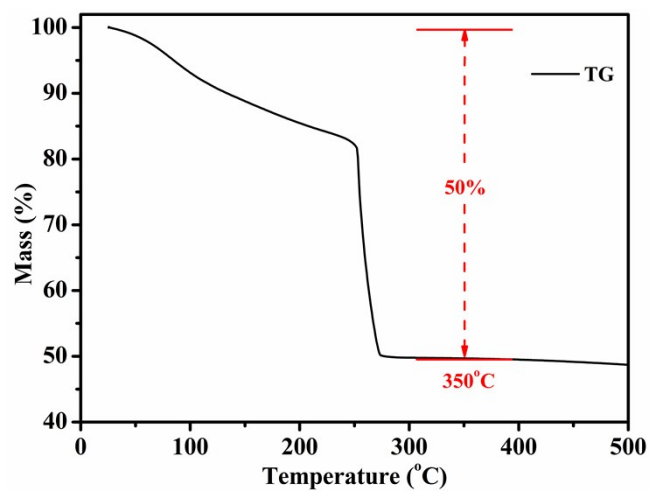
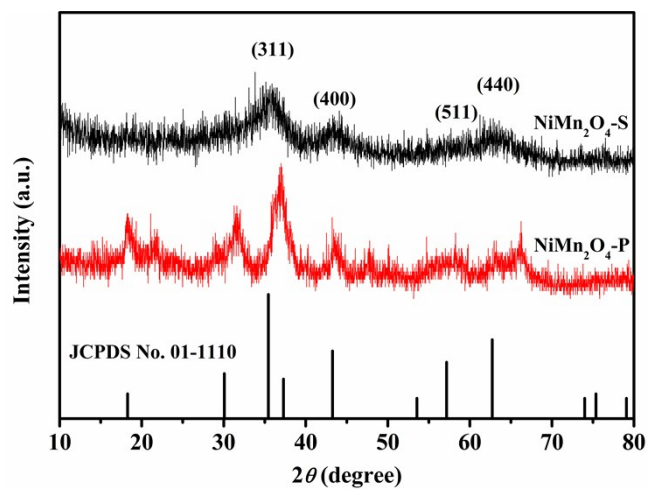**Fig. S1** TG analysis curve of the NiMn$_2$O$_4$ precursor (NiMn-glycerate).
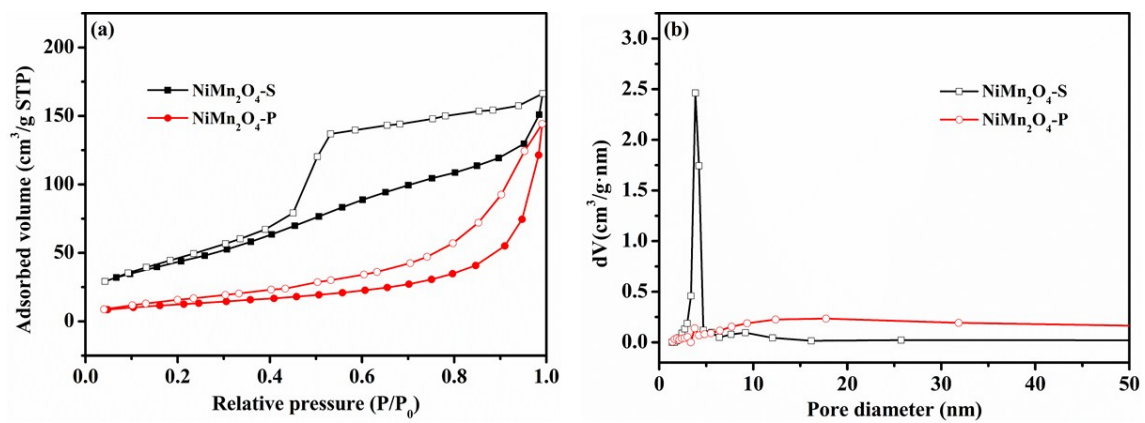
Fig. S2 XRD patterns of NiMn$_2$O$_4$ catalysts.

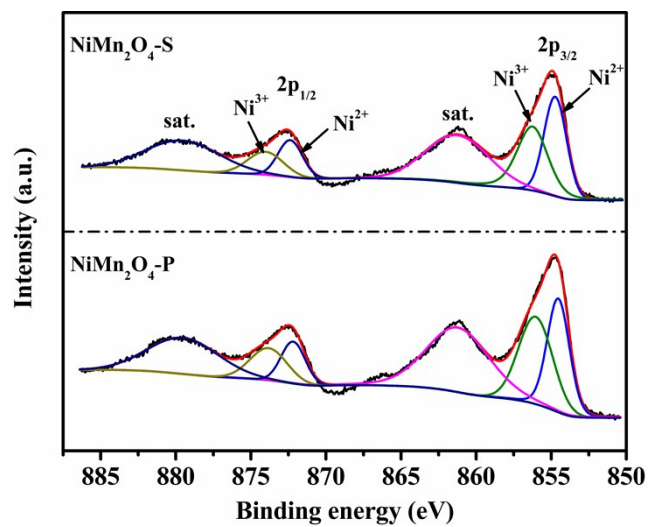**Fig. S3** (a) N_2 adsorption-desorption isotherm and (b) pore size distribution of $NiMn_2O_4$ samples.
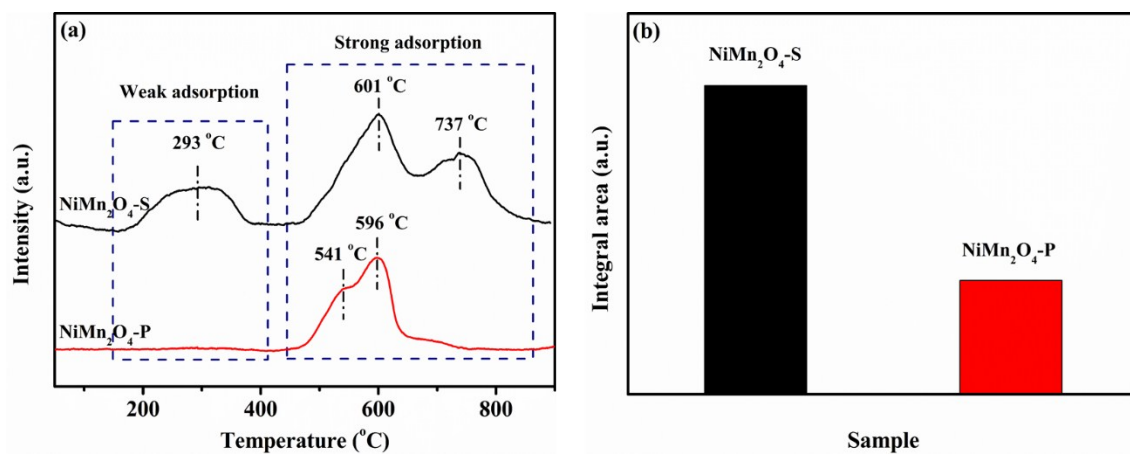
Fig. S4 XPS spectra of Ni 2p over NiMn$_2$O$_4$ catalysts.

Fig. S5 (a) NH$_3$-TPD profiles and (b) the integral area of NiMn$_2$O$_4$ catalysts.
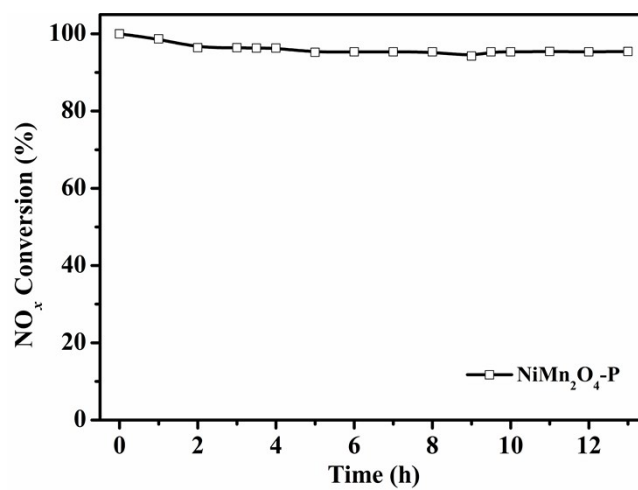
Fig. S6 Stability test of NiMn$_2$O$_4$-P catalyst at 150 °C. Reaction conditions: [NO] = [NH$_3$] = 500

ppm, [O$_2$] = 5 vol.%, balanced with Ar, GHSV = 68000 h^{-1}.

References:

1. S. K. Kaverlavani, S. E. Moosavifard and A. Bakouei, *Chem. Commun.*, 2017, **53**, 1052-1055.

2. B. Liu, X. Li, Q. Zhao, Y. Hou and G. Chen, *J. Mater. Chem. A*, 2017, **5**, 8909-8915.

3. X. Wang, Z. Lan, K. Zhang, J. Chen, L. Jiang and R. Wang, *J. Phys. Chem. C*, 2017, **121**, 3339-3349.

4. P. G. Smirniotis, D. A. Pena and B. S. Uphade, *Angew. Chem. Int. Ed*., 2001, **40**, 2479-2482.

5. P. M. Sreekanth, D. A. Pena, and P. G. Smirniotis, *Ind. Eng. Chem. Res.*, 2006, **45**, 6444-6449.

6. P. R. Ettireddy, N. Ettireddy, S. Mamedov, P. Boolchand and P. G. Smirniotis, *Appl. Catal. B*, 2007, **76**, 123-134.

7. B. Thirupathi and P. G. Smirniotis, *Appl. Catal. B*, 2011, **110**, 195-206.

8. B. Thirupathi and P. G. Smirniotis, *J. Catal.*, 2012, **288**, 74-83.

9. T. Boningari, P. R. Ettireddy, A. Somogyvari, Y. Liu, A. Vorontsov, C. A. McDonald and P. G. Smirniotis, *J. Catal.*, 2015, **325**, 145-155.

10. D. K. Pappas, T. Boningari, P. Boolchand and P. G. Smirniotis, *J. Catal.*, 2016, **334**, 1-13.

11. L. Zhang, L. Shi, L. Huang, J. Zhang, R. Gao and D. Zhang, *ACS Catal.*, 2014, **4**, 1753-1763.

12. Y. Wan, W. Zhao, Y. Tang, L. Li, H. Wang, Y. Cui, J. Gu, Y. Li and J. Shi, *Appl. Catal. B*, 2014, **148–149**, 114-122.